MINISTRY OF AVIATION

AERONAUTICAL RESEARCH COUNCIL
REPORTS AND MEMORANDA

An Extensive Theoretical Study of the Ability of Slender-Wing Aircraft to Perform Sidestep Manoeuvres at Approach Speeds

By B. N. TOMLINSON

LONDON: HER MAJESTY'S STATIONERY OFFICE

1964

PRICE 12s. 0d. NET

An Extensive Theoretical Study of the Ability of Slender-Wing Aircraft to Perform Sidestep Manoeuvres at Approach Speeds

By B. N. TOMLINSON

COMMUNICATED BY THE DEPUTY CONTROLLER AIRCRAFT (RESEARCH AND DEVELOPMENT), MINISTRY OF AVIATION

Summary.

The sidestep manoeuvre is investigated in some detail for a slender-wing aircraft by specifying the bank-angle time history and determining the required control angles. The effect of inclusion of the full inertia terms, the influence of different bank-angle time histories and the consequences of wide variations in the aerodynamic derivatives are examined. It is found that it is not necessary to include the full inertia terms in the equations of motion. An efficient manoeuvre requires a rapid initial growth of roll angle; if this is not achieved, subsequent control demands are large and only a small sidestep distance is achieved. Besides control effectiveness, the most important derivatives are the yawing moment due to aileron, the rolling moment due to rudder and the yawing moment due to rate of roll. Rudder requirements are much greater than aileron requirements. The initial demands for a good manoeuvre or subsequent demands for a poorly executed manoeuvre could be a design case for the rudder. A tentative design criterion is suggested. If the rudder is not used, the large sideslip angles which develop would require the use of excessively large aileron angles. It appears necessary to attempt some co-ordination of the manoeuvre by the use of the rudder. Piloting difficulties may be greatly alleviated by linking the rudder to the aileron.

LIST OF CONTENTS

LIST OF ILLUSTRATIONS

---

1. *Introduction.*

A sidestep manoeuvre is often necessary, when an aircraft breaks cloud at the end of an instrument approach, in order to correct a lateral displacement from the runway centre-line. Such a displacement error may be due either to the inherent limitations of the approach aid (*see* Table I of Ref. 1) or to poor following by the pilot of the guidance information. Adjustment of the flight path is usually achieved by a sequence of two banked turns, so that rolling performance is crucial.

Despite the trend towards the automation of the approach and landing, aircraft must still be capable of landing under pilot control, and must therefore have suitable characteristics for performing lateral jinks. Until recently little published work existed to guide designers in deciding exactly what aircraft characteristics best suit the manoeuvre. A series of experimental flight tests was carried out at Royal Aircraft Establishment, Bedford during 1955 and 1956 to study just those aircraft characteristics and piloting techniques which affect the performance of the correction manoeuvre. The tests used several different types of aircraft, most of which were of conventional high aspect ratio, straight wing configuration. Lean described some of the results at the 9th I.A.T.A. Technical Conference at San Remo in 1956 and a complete report has now been published[1].

Both airline and R.A.E. pilots participated in this flight study, which established that a co-ordinated S turn was the most effective method of correction and that the time required for correcting a given displacement depended mainly on the maximum rate of roll and permissible bank angle. Even for an aircraft with excellent rolling characteristics there was a minimum time of about 10 seconds for the smallest lateral correction requiring a deliberate manoeuvre. The results for a small delta-wing research aeroplane showed that, probably as a result of the aircraft's complex rolling behaviour, its performance was inferior to that expected from measurement of its maximum rate of roll.

Interest in slender configurations for supersonic transport aircraft has stimulated the theoretical study of lateral correction manoeuvres at approach speeds as a possible design case for the controls. Etkin[2] tackled the problem first, in 1959, to determine whether the large rolling moment due to sideslip characteristic of slender wings at high incidence (as on the approach) might lead to a requirement either for large aileron angles or for careful co-ordination of the controls to keep the sideslip small.

He used the conventional linearised equations of motion and neglected the effect of the shallow glide path. Preliminary analysis showed that the sidestep distance was a function of the shape of the bank-angle time history as well as of the maximum bank angle and duration of the manoeuvre. Etkin devised an anti-symmetric bank-angle function, the general shape of which was similar to some of the flight-test results. In order to preserve zero velocity and acceleration at the start of the manoeuvre and to keep the analytical function simple, he chose a form which was, in fact, less

A 2

effective than is commonly attained in practice. He recognised that the lower efficiency would reduce the distance achieved for a given bank angle but did not examine the possible effects of the bank-angle function on the control-angle requirements. The analogue computations, using early estimated and measured data for an aspect ratio one delta, included the three main cases of zero sideslip, zero rudder, and attempted suppression of sideslip by the pilot through the use of the rudder. Etkin concluded that 'the sidestep manoeuvre does not present a critical design case for the lateral controls of a slender delta aeroplane'.

Pinsker[3] followed this with a further examination of control requirements assuming a new set of derivatives and introducing at the same time inertial cross-coupling terms, pitch co-ordination and a bank-angle law more nearly in accord with practice. His main result was that, for manoeuvres co-ordinated in both pitch and yaw, peak rudder demands always exceeded peak aileron demands. He concluded that sidestep manoeuvres may be limited either by available rudder power or by the pilot's difficulty in achieving correct co-ordination. To relieve the pilot of part of the co-ordination task, Pinsker suggested a mechanical link between the ailerons and the rudder.

The significantly lower values of control effectiveness combined with adverse aileron yaw as assumed by Pinsker would clearly contribute to the difference between his main conclusions and that of Etkin; but the simultaneous changes in other derivatives, the inclusion of other terms in the equations of motion and a different bank-angle function confuse the direct comparison of results in terms of contributions from individual parameters. Because of the importance of the problem a comprehensive series of calculations was made on a Mercury digital computer to establish the influence of the various factors involved.

Both of the previous theoretical papers[2, 3] specified the manoeuvre by the bank-angle time history and determined the control-surface motions necessary to achieve this. Although this approach suppresses the aircraft 'free' dynamics it is adopted in this report to provide a basis for comparison with the previous work. When conclusions are drawn, however, the effect of dynamic problems, such as were observed with the small delta aeroplane during the flight tests[1], must not be overlooked.

After a discussion on the representation and interpretation of the results, the present work examines the effect of including the full inertia terms in the equations of motion and of attempting longitudinal co-ordination by increasing incidence with bank angle. The influence of the bank-angle function is then studied, using two extreme functions: the one suggested by Etkin[2], which is comparatively inefficient, and another which is close to the results obtained from flight tests[1] on conventional aircraft. Wide variations in the aerodynamic derivatives are made to determine which are most important. Finally, the practical limitations in terms of manoeuvre restrictions and control demands are indicated.

2. Mathematical Representation.

2.1. Equations of Motion.

The equations of motion are derived from the full Euler equations[4]. It is assumed that:

   (1) the aircraft is a rigid body;

   (2) the xz plane is a plane of symmetry;

   (3) the forward speed is constant;

   (4) the attitude perturbation from the equilibrium state is small;

   (5) the gravity term in the Z-force equation is small.

4

If the aerodynamic forces and moments are expanded in terms of the conventional linear derivatives, the equations are, for the usual wind-body axes and including *all* the terms,

$$(D - z_w)\hat{w} - \hat{q} - z_\eta \eta + \hat{p}\hat{v} = 0 \tag{1}$$

$$-\left(\frac{2\bar{c}}{b} m_{\dot{w}} D + \mu_2 m_w\right)\hat{w} + \left(\frac{b}{2\bar{c}} i_B^* D - \frac{2\bar{c}}{b} m_q\right)\hat{q} - \mu_2 m_\eta \eta +$$

$$+ \frac{b}{2\bar{c}}\{(i_A - i_C)\hat{p}\hat{r} + i_E(\hat{p}^2 - \hat{r}^2)\} = 0 \tag{2}$$

$$(D - y_v)\hat{v} + \hat{r} - \tfrac{1}{2}C_L \cos \gamma_e \sin \phi - y_\zeta \zeta - \hat{p}\hat{w} = 0 \tag{3}$$

$$-\mu_2 l_v \hat{v} + (i_A D - l_p)\hat{p} - (i_E D + l_r)\hat{r} - \mu_2 l_\xi \xi - \mu_2 l_\zeta \zeta +$$

$$+ (i_C - i_B^*)\hat{q}\hat{r} - i_E \hat{p}\hat{q} = 0 \tag{4}$$

$$-\mu_2 n_v \hat{v} - (i_E D + n_p)\hat{p} + (i_C D - n_r)\hat{r} - \mu_2 n_\xi \xi - \mu_2 n_\zeta \zeta +$$

$$+ (i_B^* - i_A)\hat{p}\hat{q} + i_E \hat{q}\hat{r} = 0 \tag{5}$$

where

$$i_B^* = \frac{B}{m\left(\frac{b}{2}\right)^2} = \left(\frac{2\bar{c}}{b}\right)^2 i_B$$

and

$$D \equiv \frac{d}{d\tau}.$$

The displacement of the aircraft relative to earth-fixed axes $Ox'y'z'$, with Oz' vertically downward and Ox' horizontal so that the initial direction of motion of the aircraft is in the plane $Ox'z'$, may be found from[4]

$$Dy' = U_0 \hat{t}\{\psi \cos \gamma_e + \hat{v} \cos \phi - \hat{w} \sin \phi\}. \tag{6}$$

If it is assumed, as in Ref. 3, that the aircraft's altitude, or rate of descent, is to remain constant, the incidence must be increased, as the aircraft banks, so that the vertical lift component is unchanged. The change of incidence necessary is given by

$$\hat{w} = \hat{w}_0 (\sec \phi - 1). \tag{7}$$

For a bank angle of about 20°, the change of incidence for a datum value of 15° is only about 1°, which is small enough to be ignored by the pilot.

There are two further kinematic equations:

$$D\phi = \hat{p} + (\hat{q} \sin \phi + \hat{r} \cos \phi) \tan \gamma_e \tag{8}$$

$$D\psi = (\hat{q} \sin \phi + \hat{r} \cos \phi) \sec \gamma_e \tag{9}$$

where the bank angle ϕ is given by

$$\phi = \phi_{\max} f(\tau).$$

Because the flight-path angle γ_e is small $(-3°)$, it is assumed (as in Refs. 2 and 3) that $\tan \gamma_e$ may be ignored and that $\sec \gamma_e$ is unity. This gives the useful result

$$D\phi = \hat{p}. \tag{8a}$$

5

To make the problem soluble, a further assumption is necessary. Each of the following is made in turn:

(1) $\hat{v} \equiv 0$, the sideslip at the c.g. is suppressed exactly;

(2) $\zeta \equiv 0$, the rudder is fixed.

Linearisation of these equations may be achieved if, firstly products such as $\hat{p}\hat{q}$ or $\hat{q} \sin \phi$ may be neglected as being of second order and secondly, the influence of the longitudinal co-ordination expressed by equation (7) is small. The five-degree-of-freedom equations then become the conventional linearised three-degree-of-freedom lateral set as used in Ref. 2.

2.2. Bank-Angle Forcing Functions.

The bank-angle forcing function employed in Ref. 2 is given by equation (10), and that in Ref. 3 by equation (11) below, where $\phi_{\max}$ is the maximum bank angle reached during the manoeuvre, duration t_3 seconds.

$$\phi = 0\cdot385\phi_{\max} \left(2 \sin \frac{2\pi}{t_3} t - \sin \frac{4\pi}{t_3} t \right) \tag{10}$$

$$\left. \begin{array}{l} 0 < t < t_1 \\ \qquad \phi = \dfrac{\phi_{\max}}{2} \left[1 - \cos \left(\dfrac{\pi t}{t_1} \right) \right] \\ t_1 < t < t_2 \\ \qquad \phi = \phi_{\max} \cos \pi \left(\dfrac{t - t_1}{t_2 - t_1} \right) \\ t_2 < t < t_3 \\ \qquad \phi = - \dfrac{\phi_{\max}}{2} \left[1 + \cos \pi \left(\dfrac{t - t_2}{t_3 - t_2} \right) \right] . \end{array} \right\} \tag{11}$$

For the roll acceleration to be continuous at t_1 and t_2

$$t_1' = t_3 - t_2 = \frac{(t - t_1)}{\sqrt{2}} .$$

These two functions are plotted in the non-dimensional form

$$\frac{\phi}{\phi_{\max}} = f(\lambda), \quad \lambda = \frac{t}{t_3} = \frac{\tau}{\tau_3} \tag{12}$$

in Fig. 1 and may also be compared with a curve obtained from flight tests[1] for a *Comet* aircraft. In Ref. 1 simple analysis using a third bank-angle function

$$\phi = \phi_{\max} \sin \frac{2\pi}{t_3} t \tag{13}$$

gives theoretical results for sidestep distances, achieved in a given time for a given maximum bank angle, which agree very well with practice. This function is also plotted in Fig. 1, which shows how very closely the flight result approximates to a sine curve.

Following Etkin the relative efficiencies of these forcing functions may be derived. Linearisation of equation (6) gives

$$Dy' = U_0\hat{t}(\psi + \hat{v}) \tag{6a}$$

and equations (9) and (3) become

$$D\psi = \hat{r} \tag{9a}$$

$$(D - y_v)\hat{v} + \hat{r} - \tfrac{1}{2}C_L\phi - y_\zeta\zeta = 0 . \tag{3a}$$

6

If equations (6a), (9a) and (3a) are combined

$$D^2 y' = U_0 \hat{t} (\tfrac{1}{2} C_L \phi + y_v \hat{v} + y_\zeta \zeta)$$

and if it is assumed that $y_v \hat{v} + y_\zeta \zeta = 0$, or is small

$$D^2 y' = \tfrac{1}{2} U_0 \hat{t} C_L \phi.$$

Integration yields

$$y' = \tfrac{1}{2} C_L U_0 \hat{t} \int_0^\tau \int_0^\tau \phi \, d\tau \, d\tau$$

and if (12) is used

$$y'_{max} = s = \frac{C_L U_0 t_3^2 \phi_{max}}{2\hat{t}} \int_0^1 \int_0^\lambda f(\lambda) \, d\lambda \, d\lambda. \tag{14}$$

The double integral in equation (14) is denoted by k. An idealised manoeuvre, in which the vehicle instantaneously attains a steady bank angle and then instantaneously reverses this bank angle half way through the manoeuvre, gives the maximum possible value of k, denoted k_0. The efficiency of a real manoeuvre may then be measured by

$$E = \frac{k}{k_0}$$

and is, in practice, determined by pilot technique. Thus

$$s = \frac{C_L U_0 \phi_{max} k_0 E t_3^2}{2\hat{t}}. \tag{14a}$$

Some values of k and E are tabulated below.

$f(\lambda)$	k	$E\%$
Flight 6, *Comet* . .	0·145	58·0
Equation (10) . .	0·092	36·8
Equation (11) . .	0·121	48·4
Equation (13) . .	0·159	63·6

Since C_L may be written

$$C_L = \hat{t} \frac{2g}{U_0}$$

equation (14a) becomes

$$s = g k_0 E \phi_{max} t_3^2 \tag{15}$$

or

$$\frac{s}{\phi_{max}} = g k_0 E t_3^2 \tag{16}$$

or, as in Ref. 2, since $d = U_0 t_3$

$$\frac{s}{\phi_{max} d} = k_0 E \left(\frac{gd}{U_0^2} \right). \tag{17}$$

For a given E and ϕ_{max}, the sidestep distance s is a function of t_3 only, and is independent of the approach speed U_0.

7

Since the efficiencies of the functions of equations (10) and (13) shown in the above table are so different it is of interest to compare how these functions and their integrals build up with time. They are plotted in Figs. 1b to 1d, which show clearly how the initial rapid growth of roll angle for the sine function contributes ultimately to a high value of the efficiency factor E.

Unfortunately, for a transition manoeuvre from one steady state to another, the sine function of equation (13) specifies an impossible situation at the start and finish of the manoeuvre, with a finite roll rate existing. A comparison of $f'(\lambda)$ and $f''(\lambda)$ for the three functions mentioned above is shown in Figs. 2a and 2b. The real-time and aerodynamic-time roll rates and accelerations are related to $f'(\lambda)$ and $f''(\lambda)$ by the following equations.

$$p = \dot{\phi} = \frac{1}{\hat{t}} D\phi = \frac{\phi_{max}}{t_3} f'(\lambda) \tag{18}$$

$$\dot{p} = \ddot{\phi} = \frac{1}{\hat{t}^2} D^2\phi = \frac{\phi_{max}}{t_3{}^2} f''(\lambda). \tag{19}$$

The function of equation (10) (Ref. 2) specifies zero roll acceleration and zero roll rate at the origin but is very slow in developing, giving a comparatively small distance; the function of equation (11)[3] requires non-zero acceleration but zero roll rate at the origin, and gives a better distance (higher E) than the first function; the sine function of equation (13) requires an acceleration impulse to generate the finite roll rate at zero time but gives a good approximation to the distances achieved in actual flight tests[1] and therefore appears to be fairly realistic—except at the origin. Control demands to give rapid initial acceleration are discussed later. Fig. 2c shows how the efficiency factor E depends on the relative balancing of initial and subsequent peak demanded accelerations.

3. Results.

3.1. Representation of Results.

The results are shown in two basic forms: as control-angle time histories, for a particular forcing function, maximum bank angle and manoeuvre duration (Figs. 3, 4, 9); and as summary curves (Figs. 5, 6, 7) where the maximum demanded control moments, rather than control angles, and distance achieved are plotted against manoeuvre duration. For comparison the results of Refs. 2 and 3 are included. Plotting control moments has two advantages: it implicitly includes any variation in the control effectiveness (l_ξ, n_ζ) and takes account of non-linearities which occur for large control deflections. The results for the present work are replotted in Fig. 8 for particular values of control effectiveness.

For the summary plots, control moment per unit bank angle is taken as the dependent variable and sidestep distance or some associated parameter as independent variable. It has been shown {equation (16)} that

$$\frac{s}{\phi_{max}} = gk_0 Et_3{}^2 \text{ (approx.)}$$

so that a given s/ϕ_{max} may result either from a manoeuvre of high efficiency and short duration (t_3) or from one of lower efficiency and longer duration. Since a short manoeuvre might demand greater control movements the higher efficiency might be thought to give the poorer performance on the basis of this criterion of equal s/ϕ_{max}. A similar objection applies to the choice of the quantity $s/\phi_{max}d$ as independent variable in Refs. 2 and 3. It follows that, for direct comparison of results,

8

the factors E and t_3 involved in s/ϕ_{max} must be separated. Since the time available in practice sets a physical limit to the manoeuvre, t_3 becomes a natural choice for independent variable. With t_3 as independent parameter, separate curves of control demand and distance achieved are plotted.

The apparent differences in control requirements between the results of Ref. 2 and Ref. 3 (e.g. Fig. 6 of Ref. 3) are much reduced if the effect of different manoeuvre efficiencies (and different approach speed) is removed by plotting against t_3 as in Figs. 6 and 7. Results of Ref. 2 and Ref. 3, together with those of the present work, are plotted against $s/\phi_{\mathrm{max}}d$ in Fig. 5 for comparison with the plots against t_3 to show this effect. Comparison of Figs. 5b and 6a will also justify the objection given above to the use of $s/\phi_{\mathrm{max}}d$ as independent variable. Since the results for the present work in Fig. 5b show a higher rudder requirement for a given $s/\phi_{\mathrm{max}}d$ with the forcing function of equation (13) than with the function of equation (10), they might be described as worse, yet the *same* results plotted in Fig. 6a against t_3 lead to the opposite conclusion.

A single curve representing overall manoeuvre effectiveness may be derived by plotting sidestep distance per unit control moment against t_3. This can be useful in cases where control moment rather than allowable bank angle is the limiting factor, but a second curve is still required to show the maximum bank angle attained during a specified manoeuvre. This method of plotting is no adopted here.

3.2. *Inertia Effects.*

To examine the influence of the full inertia effects and of longitudinal co-ordination {as expressed by equation (7)}, the calculations were performed first with the full five-degree-of-freedom equations, and then with the usual linearised three-degree-of-freedom equations. {In both cases it was assumed that equations (18) and (19) hold.} The forcing function of equation (10)[2] was used. Time histories for a 15 second manoeuvre are shown in Fig. 3 for the zero-sideslip case and $22 \cdot 5^\circ$ maximum bank angle. Although there are differences they are so small as to be unimportant. It is interesting that the peak control angles for three degrees-of-freedom are slightly greater (*sic*) than for five degrees-of-freedom. In the case of the rudder, this is because at the peak the $\hat{p}\hat{q}$ term is negative. Even for the excessively large maximum bank angle of 45°, peak control angles are not very different in the two cases (*see* Fig. 4) although the time histories are distinctly different*.

Since the summary plots of Figs. 5, 6 and 7a show that the points for three degrees-of-freedom and five degrees-of-freedom lie virtually on one curve, for all subsequent analysis the three-degree-of-freedom approach is used.

3.3. *The Specified Manoeuvre.*

The choice of bank-angle forcing function is important for two reasons. Firstly, the sidestep distance achieved in a given time and for a given maximum bank angle is approximately proportional to E, which depends on the double integral of the bank-angle curve. Secondly, the maximum demanded control moment is approximately proportional to the maximum demanded acceleration which depends on the 'peakiness' of the bank-angle curve. For both these reasons different forcing functions can be expected to introduce differences between sets of results which obscure both the influence of the aerodynamic assumptions and the conclusions to be drawn from the graphs.

---

* This is in contradiction to Ref. 3, which attributed a large factor in the differences between Ref. 2 and Ref. 3 to the inclusion of the full inertia terms and to longitudinal co-ordination.

To clarify these points, control demands have been computed, using the aerodynamic data of the present work, for the forcing functions of equations (10), (11) and (13) for a manoeuvre of 15 seconds duration and ϕ_{max} of $22 \cdot 5°$ (Fig. 9). It is clear from Fig. 9 that correction for the effect of the forcing function would increase still further the differences between the conclusions of Refs. 2 and 3 regarding maximum demanded control angles.

Summary plots for different manoeuvre durations are shown in Figs. 6 and 7, for the forcing functions of equations (10) and (13) only, together with the results of Refs. 2 and 3. Not only are the control moments reduced with the function of equation (13), as compared with equation (10), but the sidestep distance for a given time is also much increased. The summary plot of Fig. 5 is included only as a reference to the earlier criterion $(s/\phi_{max}d)$, and to show, by comparison with Fig. 6, the inversion of the results with the forcing functions of equations (10) and (13). As might be expected, the results of Ref. 3 lie between those for equation (10) and equation (13) (Figs. 6 and 7). The lower control requirements of Ref. 2 compared with the present work using the same forcing function {equation (10)} are due to the different aerodynamic characteristics assumed.

The present results are replotted in a slightly simpler form, in terms of control angles and sidestep distances, in Fig. 8. Since the aerodynamic data are the same in each case, the differences between the two sets of rudder (and aileron) results in Fig. 8a are due solely to different maximum demanded roll rates and accelerations, while in Fig. 8b the difference in sidestep distance achieved is due solely to a different value of E. All distances are obtained by integration of equation (6).

Although the results in Figs. 6, 7 and 8 for the sinusoidal forcing function of equation (13) show a desirable reduction in control moments compared with the function of equation (10), it should be remembered that the sine function has peculiar characteristics at the origin, since the maximum roll rate exists at the beginning. Physically, an acceleration impulse would be necessary to generate a finite roll rate* in zero time, which is not possible, but since near sinusoidal bank-angle time histories can be achieved[1], it is assumed that such a bank-angle function is justified, without involving the pilot in any extraordinary behaviour. The sidestep distances achievable in practice will approximate those shown for equation (13) only if the aircraft is capable of building up this roll rate in the first second or so of the manoeuvre. In doing so the maximum control demands may well be greater than those plotted. This is considered in Section 4 on manoeuvre limits.

3.4. Derivatives.

Wind-tunnel tests on slender shapes, more recent than those available for Ref. 3, indicate that a sensible set of data is as given in Table 1 at the end of the report. Included in the same table for comparison are the data used in Refs. 2 and 3. Most of the derivatives used in Ref. 2 were estimated, while most of those used here and in Ref. 3 were based on wind-tunnel tests.

It has been found by a large number of variations that, in addition to the control powers, the two derivatives which have a big influence on the magnitudes of the peak control angles necessary to manoeuvre are the cross derivatives l_ζ (the rolling moment due to rudder) and n_ξ (the yawing moment due to aileron). This may be seen in Fig. 10a where peak control angles, expressed as a proportion of the maximum bank angle, are plotted for various values of l_ζ and n_ξ, while all other derivatives were kept fixed. In this report the basic values used are $l_\zeta = 0$, $n_\xi = 0$ but Etkin in Ref. 2 assumed the optimistic value of $n_\xi = -0 \cdot 025$ (with $l_\zeta = 0$) while Pinsker in Ref. 3 was

---

* This finite roll rate is given by $2\pi\phi_{max}/t_3$, and equals $9 \cdot 4°/\text{sec}$ for $\phi_{max} = 22 \cdot 5°$ and $t_3 = 15$ sec.

pessimistic and took $n_\xi = +0 \cdot 03$ (also with $l_\xi = 0$). It is interesting to note that even with $l_\xi = +0 \cdot 02$ and $n_\xi = -0 \cdot 02$ the ratio of peak rudder angle to peak aileron angle is greater than unity. This is still true if the rudder and aileron powers are reduced respectively to $-0 \cdot 06$ and $-0 \cdot 07$. This rudder to aileron ratio is found to be independent of the shape of the forcing function and therefore depends only on the aircraft data, in particular on the inertias and on the control derivatives.

The yawing moment due to aileron, n_ξ, may have two components if both inboard and outboard ailerons are used to roll the aircraft (the inboard ailerons also serving as elevators). Positive aileron deflection (starboard aileron down) rolls the aircraft to the left. For simple flap-type ailerons, the increase in lift on the right wing and decrease on the left produce a drag differential which gives a yawing moment to the right, which is 'adverse' and n_ξ is positive. Positive deflection of the control surfaces immediately adjacent to the fin, however, induces an extra sideforce on the fin which yaws the aircraft to the left, making this contribution to n_ξ negative. In this report it is assumed that these two components are equal, so that the gross value of n_ξ is zero. It is worth noting that although the inboard ailerons do not contribute much to the rolling power, they may help indirectly by producing a 'favourable' yawing moment.

Of the other derivatives, the roll damping, l_p, and the yawing moment due to rate of roll, n_p, have most effect on the peak control angles, as shown in Fig. 10b, while the influence of the damping-in-yaw, n_r, and the rolling moment due to rate of yaw, l_r, is slight. Some recent wind-tunnel results indicate that the value of n_p may be lower than was at first expected. At 15° incidence the value of n_p may be as low as $-0 \cdot 027$, which would reduce the rudder requirements immediately by about one sixth as compared with the value assumed in the calculations. Any artificial roll damping, which has been suggested would improve the response to a sidegust, naturally would oppose a manoeuvre of the kind discussed in this work.

3.5. *Rudder and Aileron Requirements.*

Typical time histories (e.g. Fig. 9) show that maximum rudder angles required are greater than maximum aileron angles. This unusual feature of the slender delta aircraft, which is due to its high inertia in yaw, will displease pilots who point out[1] that, among the factors affecting manoeuvres during the landing approach, 'control harmony' is important.

Even if large sideslip angles could be tolerated by the structure it would not be possible to perform a sidestep manoeuvre without using the rudder, because of the extreme aileron angles necessary to overcome the large rolling moments due to sideslip. A typical time history is shown in Fig. 11a but it should be noted that since the aircraft does not return to the equilibrium state by the end of the manoeuvre the results, a summary of which is shown in Fig. 12, should be used with care. These results indicate how necessary it is to co-ordinate the manoeuvre and keep the sideslip, $\hat{v}$, small. Since the magnitudes of the maximum sideslip and aileron angles developed in the present work are several times those of Ref. 2, the analogue-computer results of Ref. 2 were checked directly (with the same assumptions as in Ref. 2) on the digital computer. It was found that they were in error, but the source of the error is not known. The corrected values are shown in Fig. 12.

By incorporating a direct link, as suggested by Pinsker[3], between aileron and rudder, so that when the aircraft is rolled, the rudder is automatically moved an appropriate amount to minimise sideslip, the piloting problems may be reduced. This aileron-rudder gearing can be a simple (but one way) link because, as is evident from Figs. 3 and 9, rudder and aileron movements are similar

in phase. Fig. 11b shows a plot of control angles required and sideslip developed with a straight gearing of $1 \cdot 70$. This gearing is equivalent to a ratio of required control moments of $1 \cdot 33$, which would be the actual gearing necessary if the aileron power were equal to the rudder power. Simple calculations for approaches at constant weight but varying incidence show that a constant gearing would be adequate. Control demands are reduced with decreasing incidence but the relation between rudder and aileron requirements does not vary.

An illustration of the fundamentally complex rolling behaviour of delta aircraft, mentioned in the Introduction, is given in Fig. 13 which shows the response of a slender delta to a step-aileron movement. It may be seen in the figure that with a rudder-aileron gearing of $1 \cdot 70$ the undesirable bank-angle oscillation is nearly eliminated.

4. Manoeuvre Limitations.

4.1. Manoeuvre Time.

Since Ref. 1 found that the minimum time to correct a displacement of significant magnitude was about 10 seconds, the minimum practical manoeuvre distance, d, is between 2000 (120 kt) and 2500 ft (150 kt) depending on approach speed. For a break-off height of 300 ft, a 3° glide path and for the sidestep manoeuvre to be completed before the beginning of the flare at 50 ft, the maximum distance available for manoeuvring is about 5000 ft. At 150 knots, this distance is equivalent to a manoeuvre time of 20 seconds. If the pilot establishes contact with the ground at a height greater than 300 ft he will, of course, have available a greater distance than 5000 ft in which to manoeuvre.

4.2. Bank Angle.

Under manual control near the ground a large transport aircraft will not normally be banked to angles greater than 20 to 30° except during an emergency. This upper limit of 30° has been tentatively suggested by the flight tests reported in Ref. 1. A representative figure of 20° is used in Fig. 14.

4.3. Control Effectiveness.

Since it has been shown that the required rudder moment is greater than the required aileron moment, the sidestep ability will be limited by the rudder rather than by the aileron, unless the available rudder moment is greater than the available aileron rolling moment.

According to some unpublished wind-tunnel data on control moments at zero sideslip, the maximum rudder moment $(C_n)_{\max}$ available on one model is about $0 \cdot 028$ and the maximum rolling moment due to the ailerons, $(C_l)_{\max}$, is about $0 \cdot 035$. These values would limit the maximum bank angle which could be used for manoeuvring. Fig. 7b shows the relationship between $(C_n)_{\max}$ {or $(C_l)_{\max}$} and $(C_n)_{\max}/\phi_{\max}$ {or $(C_l)_{\max}/\phi_{\max}$} for various values of maximum bank angle, thus enabling the results of Fig. 6 or Fig. 7a to be interpreted in terms of design requirements for the rudder or aileron if the maximum bank angle is specified.

If, for $(C_n)_{\max} = 0 \cdot 028$, the rudder power $n_\zeta = -0 \cdot 06$ (a rather more pessimistic value than has been used in the calculations) the 'equivalent' maximum rudder deflection is 27°*, but since a pilot would not like having to use the full rudder deflection, the useful maximum is only about

---

* The curve of rudder moment against deflection is not linear for large deflections, so that the total yawing moment, $(C_n)_{\max}$, due to the rudder is equal to the rudder power n_ζ times the 'equivalent' maximum deflection and not to the rudder power times the actual maximum deflection.

20°. The results replotted in Fig. 8 for $n_\zeta = -0\cdot06$ show that, with the forcing function of equation (13) and for a manoeuvre duration of 10 seconds, ζ_{max}/ϕ_{max} is about $0\cdot9$. This means that if ϕ_{max} is 20°, the required rudder angle is 18°, which is just within the useful limit of 20°. The initial impulse required to achieve this function demands control moments similar in magnitude to those plotted for the peak values of the manoeuvre of equation (10) and would limit ϕ_{max} to 12° and sidestep distance to about 120 ft. For the low-efficiency forcing function of equation (10) bank angle is again limited to 12° but sidestep distance would only be about 60 ft.

4.4. *Sidestep Performance.*

Fig. 14 shows the limitations of sidestep performance for poor {forcing function of equation (10)} and good {forcing function of equation (13)} manoeuvres, with restrictions on the maximum bank angle and maximum rudder angle of 20°. A poor manoeuvre becomes limited by the rudder (curve A) rather than by bank angle (curve B) at a distance of 4700 ft from the glide-path origin, allowing just under 15 seconds for a correction manoeuvre to be made, if such manoeuvre must be completed by the time the aircraft reaches a height of 50 ft.

Flight tests and the results of the present analysis show that the good manoeuvre of curve C ($E = 63\cdot6\%$) is not unrealistic. To approximate to this manoeuvre it is necessary to build up the initial roll rate, which corresponds to the required ϕ_{max} and t_3, as quickly as possible (within about $0\cdot1t_3$), with a near-step input on controls. When the manoeuvre is bank angle limited, as curve C of Fig. 14, the optimum piloting technique appears to be to use about 15% more control initially than subsequently, to give a high-efficiency manoeuvre. But because the maximum rolling acceleration is limited, a high-efficiency manoeuvre of *short* duration can only be achieved by reducing the bank angle to less than 20°. For a usable C_n of $0\cdot021$, this is necessary (point C_1) at about 4300 ft from touchdown ($t_3 = 13$ sec). Once control effectiveness rather than bank angle sets the limit on sidestep distance, a better utilisation of the controls is possible by using equal maxima at all stages. Although such a technique produces a manoeuvre, similar to that in Ref. 3, which is less efficient for a given ϕ_{max} (curve D, Fig. 14) it does enable a bank angle of 20° to be achieved for manoeuvre times down to 10 sec (curve E), giving a sidestep distance of 130 ft. The practical limiting curve in Fig. 14 then becomes C C_1 C_2.

A tentative design criterion may be derived on the basis of the initial acceleration required to achieve a manoeuvre of moderate efficiency for a manoeuvre duration of 10 seconds. Fig. 2c shows that, for the 'optimum' manoeuvre ($E = 52\%$), the value of the first peak of non-dimensional rolling acceleration, $f''(\lambda)$, needs to be about 65 to 70. Assuming that the roll rate is small, the control moment equated to the acceleration gives, for zero sideslip,

$$C_l = \frac{i_A}{\mu_2} D^2\phi = \frac{i_A}{\mu_2} \hat{t}^2 \frac{\phi_{max}}{t_3{}^2} f''(\lambda)$$

$$C_n = -\frac{i_E}{\mu_2} D^2\phi = -\frac{i_E}{\mu_2} \hat{t}^2 \frac{\phi_{max}}{t_3{}^2} f''(\lambda).$$

For the data of Table 1, and with $\phi_{max} = 20°$, $t_3 = 10$ sec and $f''(\lambda) = 65$, these expressions give $C_l = 0\cdot017$, $C_n = 0\cdot022$. With a 25% allowance for reserves, $C_l = 0\cdot021$ and $C_n = 0\cdot027$. The rudder requirement is marginally within the previously quoted figure of $0\cdot028$ (Section 4.3) and emphasises the need to establish the practicability of an efficient piloting technique.

Curve C approximates closely to the corresponding curve in Fig. 9 of Ref. 3: the lower approach speed used there (224 ft/sec, 133 kt) counteracts the lower efficiency ($48\cdot4\%$).

13

5. *Conclusions.*

An extensive theoretical study is made to determine which factors most influence the ability of a slender aircraft to perform sidestep manoeuvres during the landing approach. The results allow the effects of aircraft and manoeuvre parameters to be assessed readily in terms of the resulting sidestep distances and control requirements.

It is found that it is not necessary to use the full five-degree-of-freedom equations of motion when calculating the results because inclusion of the full inertia terms and of longitudinal co-ordination makes no significant difference to the answers.

In the estimation of control angles required to obtain a specified bank-angle response, two forcing functions are used. The initial demands for a good manoeuvre or subsequent demands for a poor one could be a design case for the rudder. Which of the forcing functions is more realistic depends on the piloting technique, but for maximum sidestep correction a high initial rate of application of controls is essential. A tentative design criterion for the controls is suggested on the basis of the initial acceleration required to achieve an optimum manoeuvre.

Plotting the results against the sidestep parameter $s/\phi_{\max}d$ may be misleading. It is thought to be more informative if the manoeuvre time t_3 is used as independent variable.

It is found that, for zero sideslip, the most severe control demands are on the rudder. If the rudder is not used, the rolling moment due to sideslip requires the use of very large aileron angles (more than double the values for zero sideslip) to roll the aircraft. It is therefore essential to use the rudder to suppress sideslip. Piloting difficulties may be greatly alleviated by employing a direct, one way, link between aileron and rudder which moves the rudder an appropriate amount to suppress sideslip as the aircraft banks.

The factors which have most influence on the actual magnitudes of the rudder demands are the control cross-derivatives, yawing moment due to aileron n_ξ, and rolling moment due to rudder l_ζ; the yawing moment due to rate of roll n_p; the yaw inertia i_C and the product of inertia i_E. Relative to the values assumed here, an unfavourable combination of n_ξ and l_ζ could increase the rudder requirements by 20% and the aileron requirements by 40%, while a favourable combination could decrease the rudder demand by 10% and the aileron demand by 30%. A reduced value of $-n_p$ could greatly reduce the rudder requirements. An intensive study to obtain reliable data on n_p for slender shapes would be worthwhile.

Since it is shown that the rudder angles required are very high and that the results depend on the pilot's technique, it would be useful either to obtain some flight-test results for large swept-wing aircraft or to use a simulator to indicate whether the aircraft dynamics, suppressed by the analytical technique used in this report, influence the pilot's ability to perform sidestep manoeuvres at approach speeds.

14

LIST OF SYMBOLS

b		Span
$\bar{c}$		Aerodynamic mean chord
C_L		Lift coefficient
$(C_l)_{\mathrm{max}}$		Maximum rolling moment due to ailerons
$(C_n)_{\mathrm{max}}$		Maximum yawing moment due to rudder
D	$\equiv$	$\dfrac{d}{d\tau}$, differential operator
d	$=$	$U_0 t_3$, longitudinal distance travelled during manoeuvre
E		Manoeuvre efficiency factor
$f(\lambda)$		Normalized function {equation (12)}
g		Gravity
i_A, i_B, i_C, i_E		Inertia coefficients†
$i_B{}^*$	$=$	$\left(\dfrac{2\bar{c}}{b}\right)^2 i_B$
k		Bank-angle shape parameter
k_0		Value of k for idealised manoeuvre
$l_p, l_r, l_v, l_\xi, l_\zeta$		Non-dimensional rolling-moment derivatives†
$m_q, m_w, m_{\dot{w}}, m_\eta$		Non-dimensional pitching-moment derivatives†
$n_p, n_r, n_v, n_\xi, n_\zeta$		Non-dimensional yawing-moment derivatives†
p, q, r		Angular velocities in roll, pitch and yaw†
$\hat{p}, \hat{q}, \hat{r}$	$=$	$p\hat{t}, q\hat{t}, r\hat{t}$
S		Wing area
s		Lateral distance moved during manoeuvre
t_3		Duration of manoeuvre (sec)
t_1, t_2		Parameters in equation (11)
t		Natural time (sec)
$\hat{t}$		Unit of aerodynamic time†

---

† Defined in R.Ae.Soc. Data Sheets Aircraft 00.00.02.

U_0 Equilibrium flight speed

v Velocity in y-direction†

$\hat{v}$ $=$ $\dfrac{v}{U_0}$, sideslip angle

W Weight

$\hat{w}$ $=$ $\dfrac{w}{U_0}$, incremental incidence

$\hat{w}_0$ $=$ $\tan \alpha_0$

y' Lateral distance relative to space-fixed axes $Ox'y'z'$

$y'_{\max}$ $=$ s

$y'_v, \, y_\zeta$ Non-dimensional lateral force derivatives†

$z_w, \, z_\eta$ Non-dimensional force derivatives†

α_0 Equilibrium incidence

γ_e Equilibrium flight-path angle

ζ Rudder angle

η Elevator angle

λ $=$ $\dfrac{t}{t_3} = \dfrac{\tau}{\tau_3}$

μ_2 Lateral relative-density parameter†

ξ Aileron angle

ρ Air density

τ Aerodynamic time

τ_3 $=$ $\dfrac{t_3}{\hat{t}}$, duration of manoeuvre in air seconds

ϕ Bank angle

$\phi_{\max}$ Maximum bank angle

ψ Yaw angle

---

† Defined in R.Ae.Soc. Data Sheets Aircraft 00.00.02.

REFERENCES

No.	Author(s)	Title etc.

1   D. H. Perry, W. G. A. Port and   A flight study of the sidestep manoeuvre during landing.
J. C. Morral   A.R.C. R. & M. 3347. July, 1961.

2   B. Etkin   An analytical study of the ability of a slender delta-wing aeroplane
                                    to perform a sidestep manoeuvre at low speed.
                                    R.A.E. Tech. Note Aero. 2623.
                                    A.R.C. 21 503. May, 1959.

3   W. J. G. Pinsker   Further consideration of the control requirements for a slender
                                    delta aircraft to perform sidestep manoeuvres at approach
                                    speeds.
                                    R.A.E. Tech. Note Aero. 2735.
                                    A.R.C. 22 822. January, 1961.

4   B. Etkin   *Dynamics of Flight.*
                                    John Wiley & Sons, New York. 1959.

TABLE 1

Aircraft Data

All derivatives are for wind-body axes

	Present work	Ref. 2	Ref. 3	
W/S	44·0	40·0	30·5	lb/ft²
U_0	253	259	224	ft/sec
C_L	0·578	0·50	0·50	
α_0	15·6	15·0	15·0	degrees
$\bar{c}$	76·4		80	ft
b	80	75	80	ft
μ_2	14·37	13·93	10·0	
$\hat{t}$	2·27	2·02	1·78	
i_A	+0·207	+0·159	+0·130	
i_B	+0·27	—	—	
i_C	+0·995	+0·941	+0·938	
i_E	−0·265	−0·222	−0·230	
$i_B{}^*$	+0·985	—	+0·92	
z_w	−1·295	—	—	
z_η	−0·306	—	—	
m_w	−0·0335	—	−0·02	
m_q	−0·198	—	−0·096	
$m_{\dot{w}}$	−0·049	—	−0·024	
m_η	−0·107	—	−0·055	
l_p	−0·141	−0·094	−0·114	
l_r	+0·250	+0·119	+0·023	
l_v	−0·166	−0·244	−0·233	
l_ξ	−0·101	−0·100	−0·054	
l_ζ	0·00	0·00	0·00	
n_p	−0·143	+0·012	−0·076	
n_r	−0·210	−0·333	−0·406	
n_v	+0·136	+0·20	+0·145	
n_ξ	0·00	−0·025	+0·030	
n_ζ	−0·079	−0·087	−0·073	
y_v	−0·182	−0·083	−0·20	
y_ζ	+0·0645	+0·158	+0·05	

Note: The computations in Ref. 3 were made in principal inertia axes. Certain corrections have been made to the equivalent derivatives for wind-body axes listed in Ref. 3.
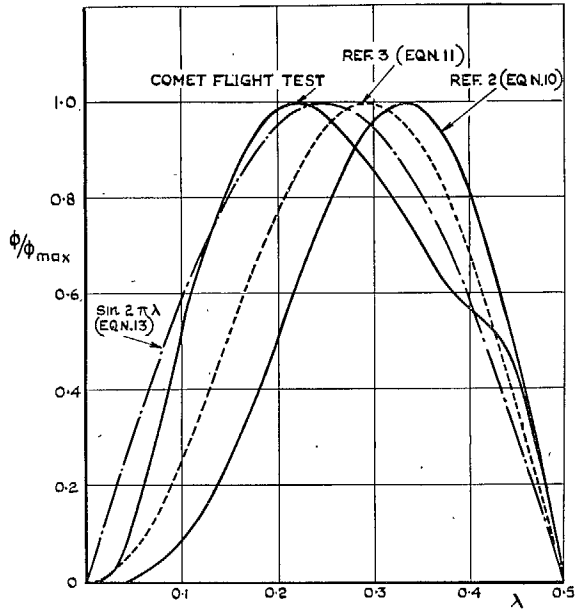
FIG. 1a. Comparison of bank-angle functions.

---- $f(\lambda) = 0.385 \; (2 \sin 2 \pi \lambda - \sin 4 \pi \lambda)$ AFTER REF. 2.

—— $f(\lambda) = \sin 2 \pi \lambda$ AFTER REF. 1.

—·—·—   IDEALISED, ZERO INERTIA, ZERO DAMPING.
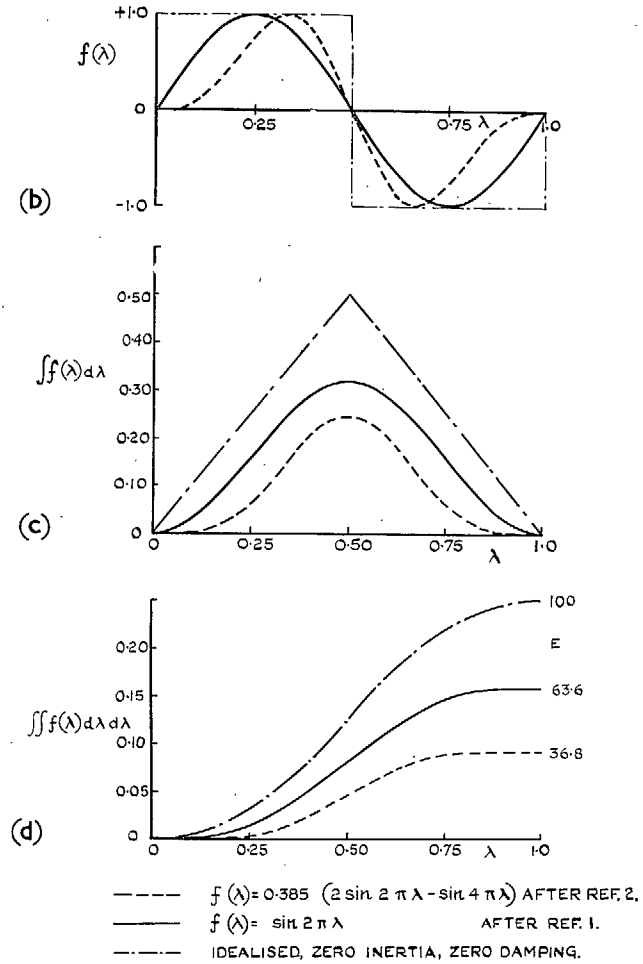
FIG. 1b to d.   Comparison between poor and good manoeuvres, in non-dimensional form.

$$f'(\lambda) = \dot{\phi}\, \frac{t_3}{\phi_{max}}$$
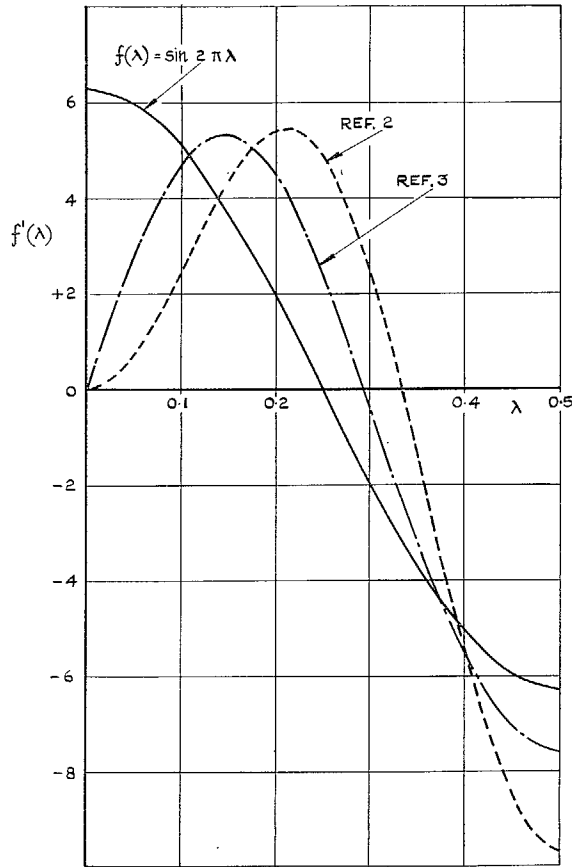
FIG. 2a.   Comparison of demanded roll rates.

$$f''(\lambda) = \ddot{\phi}\, \frac{t_3^2}{\phi_{max}}$$
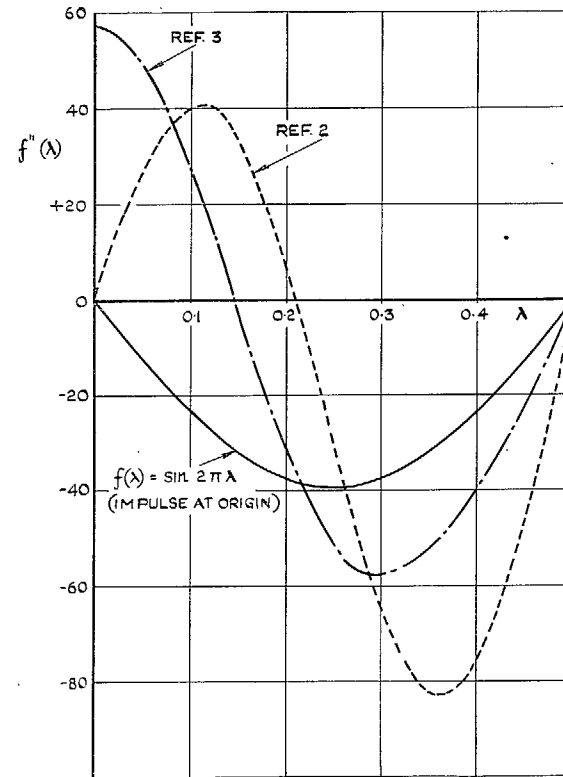
FIG. 2b.   Comparison of demanded roll accelerations.
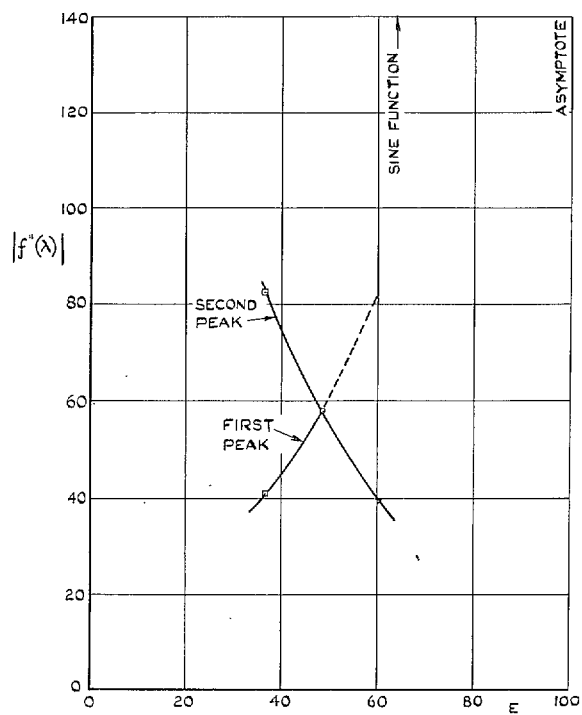
FIG. 2c. Non-dimensionalised peak rolling accelerations, $f''(\lambda)$, as a function of sidestep efficiency factor.

21
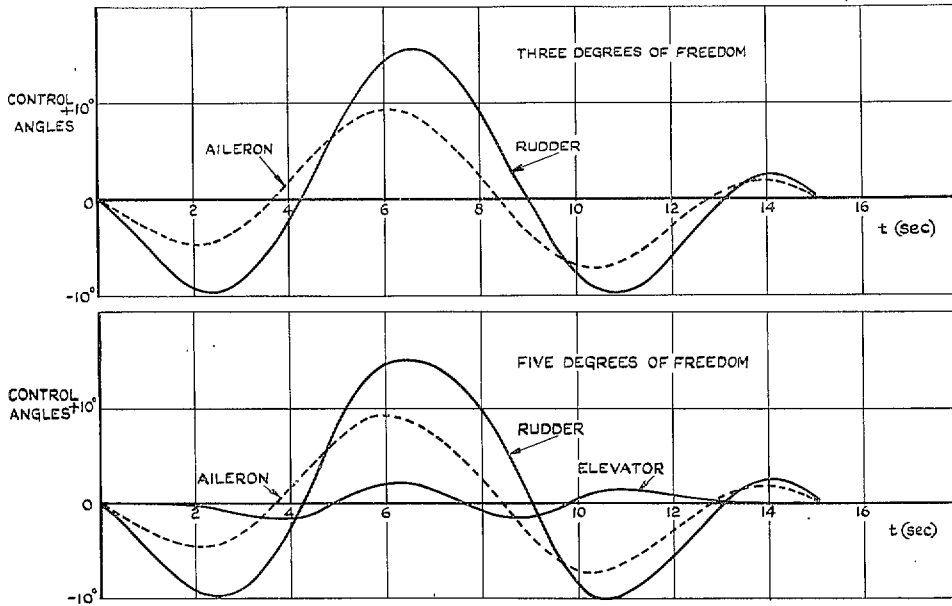
FIG. 3.   Control time histories for 22·5° bank angle, zero sideslip, forcing function of equation (10).
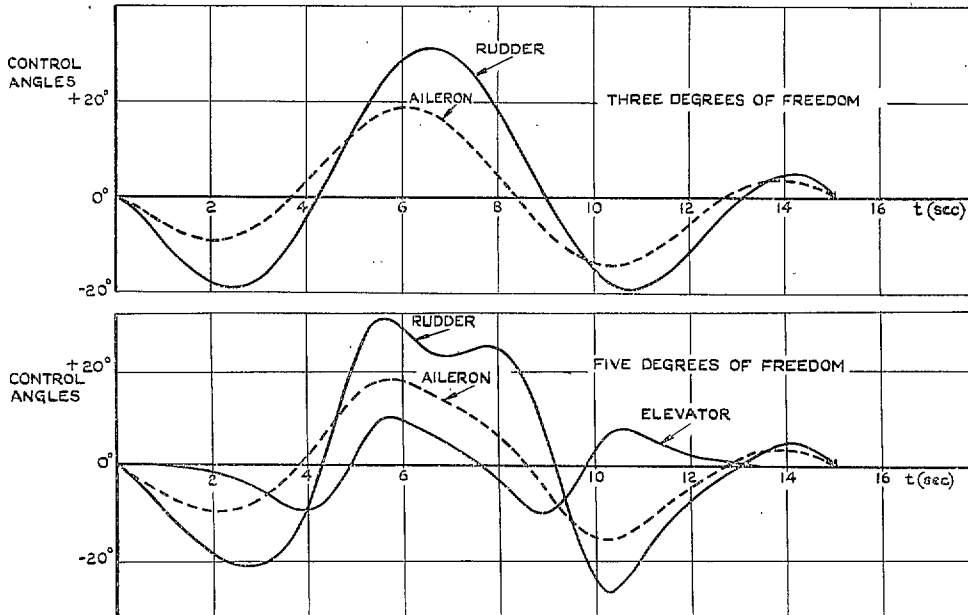
FIG. 4.   Control time histories for 45° bank angle, zero sideslip, forcing function of equation (10).
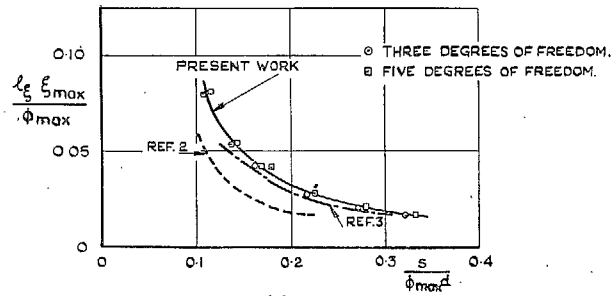
22
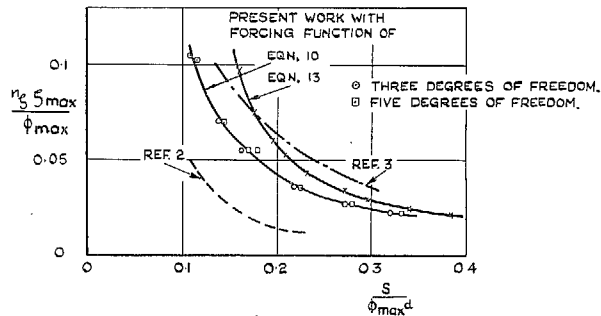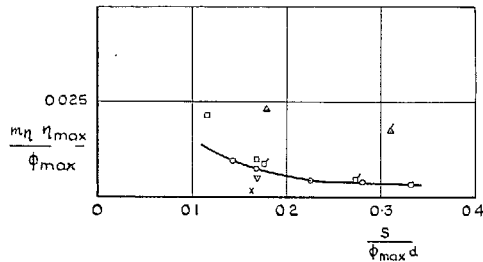
FIG. 5. Maximum control requirements for zero sideslip plotted against sidestep parameter, $s/\phi_{max}d$.
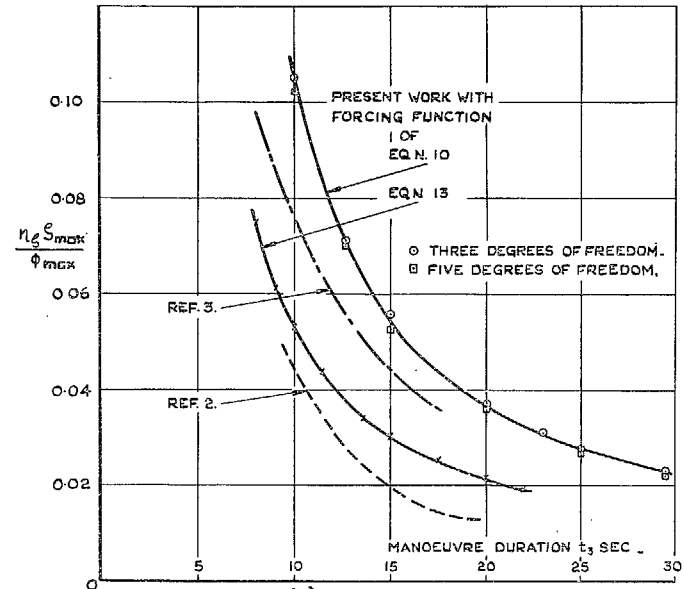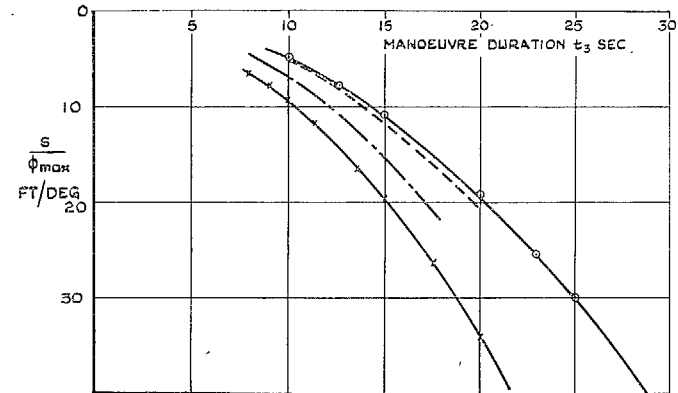
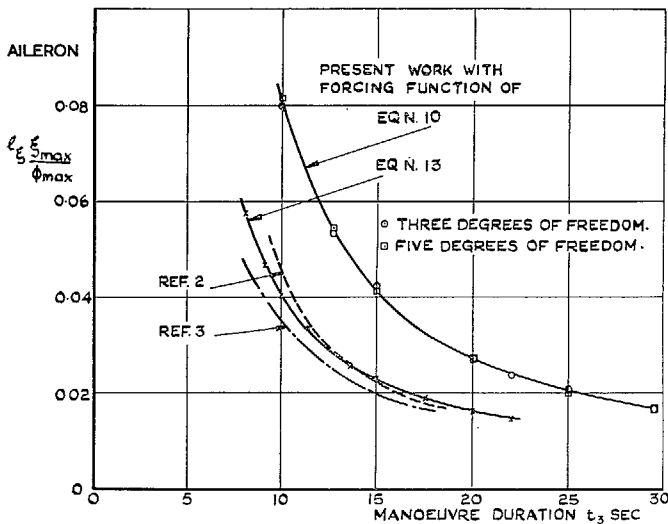FIG. 6. Rudder requirements for zero-sideslip manoeuvres.

FIG. 7a. Aileron requirements for zero-sideslip manoeuvres.

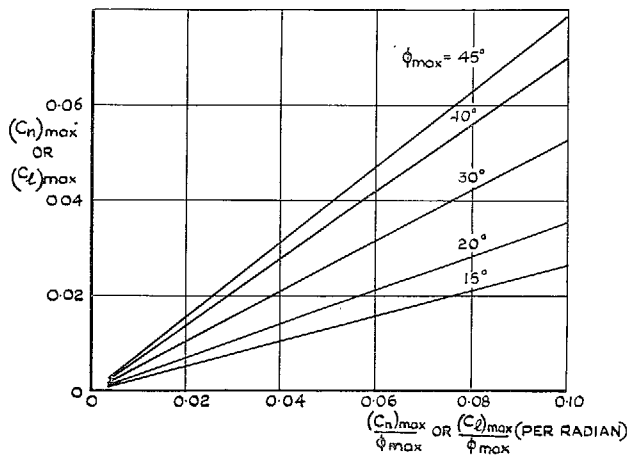

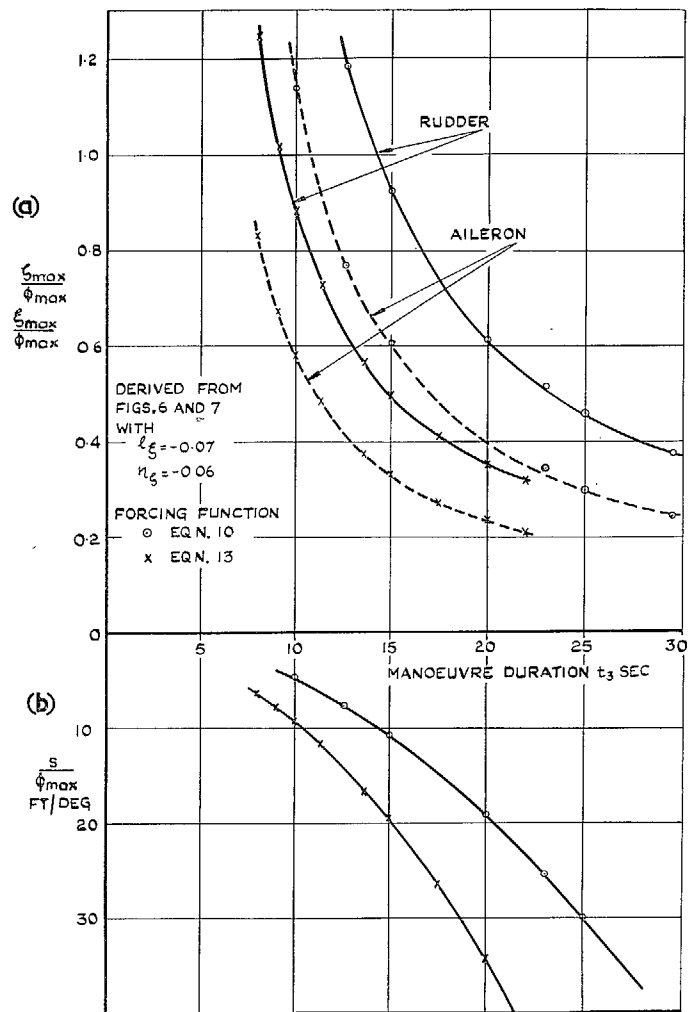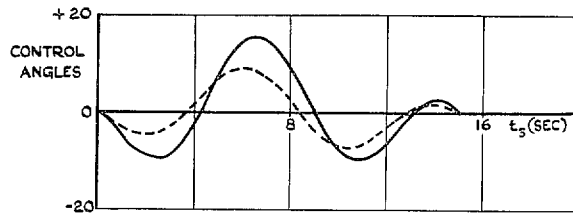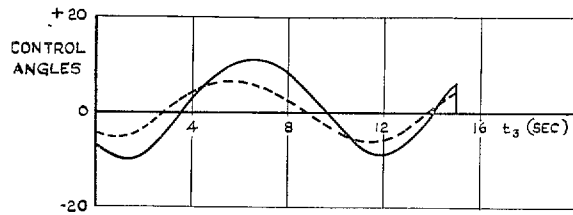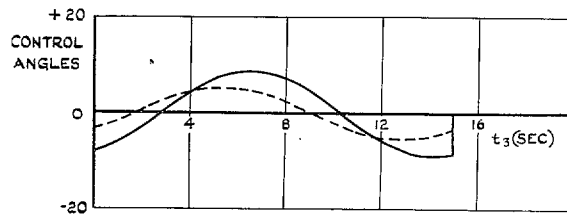FIG. 7b. Relation between $(C_n)_{max}$ and $(C_n)_{max}/\phi_{max}$.

FIG. 8. Results of present work for two forcing functions. Zero sideslip.

(a) EQUATION 10-REF. 2.

(b) EQUATION 11 -REF. 3.

(c) EQUATION 13 - REF. 1.

IN EACH CASE, $\phi_{max} = 22.5°$, $t_3 = 15$ SEC, AERODYNAMIC DATA OF PRESENT WORK AS TABLE 1.

———— RUDDER ANGLE.
— — — — AILERON ANGLE.

FIG. 9. The effect of different forcing functions.

25
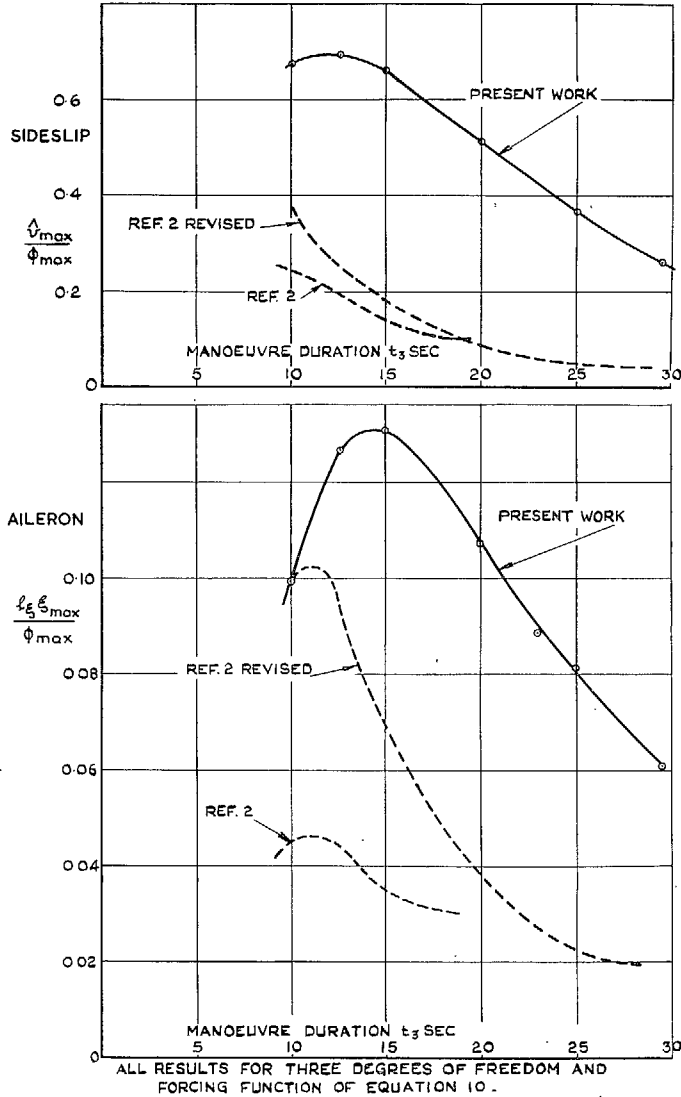
FIG. 12. Aileron and sideslip angles for rudder-fixed manoeuvres.
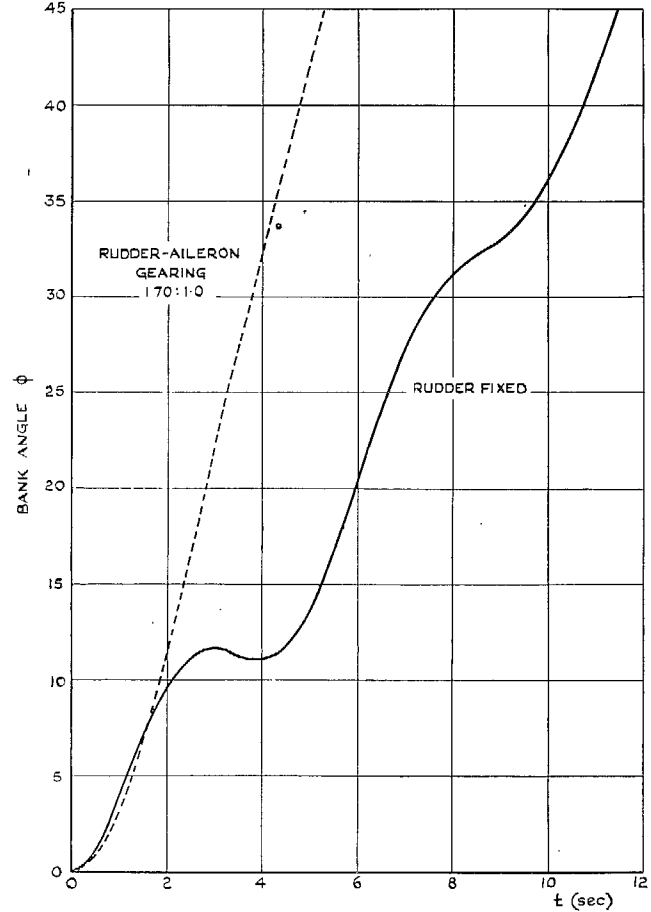
FIG. 13. Typical bank angle response to 5° step-aileron movement.

BREAK OUT AT 300FT.

POOR MANOEUVRE
(EQN. 10, E = 368%)

ϕ=20° B

A ζ= 20°

3°

500

HEIGHT (FT)

0

500

END OF
SIDESTEP

RUNWAY

8000   7000   6000   5000   4000 C₂   2000   1000   0
DISTANCE FROM GLIDE PATH ORIGIN (FT)

2000   1000   0

INITIAL FLIGHT PATH PARALLEL
TO RUNWAY.
ℓ_ξ= -0.07
n_ξ = -0.06
APPROACH SPEED 150 KT

D
ϕ= 20°(E=52%)

C
ϕ= 20°

GOOD MANOEUVRE
(EQN. 13, E=63.6%)

E

'OPTIMUM' CONTROL LIMITED
MANOEUVRE, ζ=20°(E=52%)

10 SEC

EXPERIMENTAL POINTS (REF. I) FOR
VISCOUNT, APPROACH SPEED 120 KT

500

LATERAL
DISPLACEMENT(FT)

1000

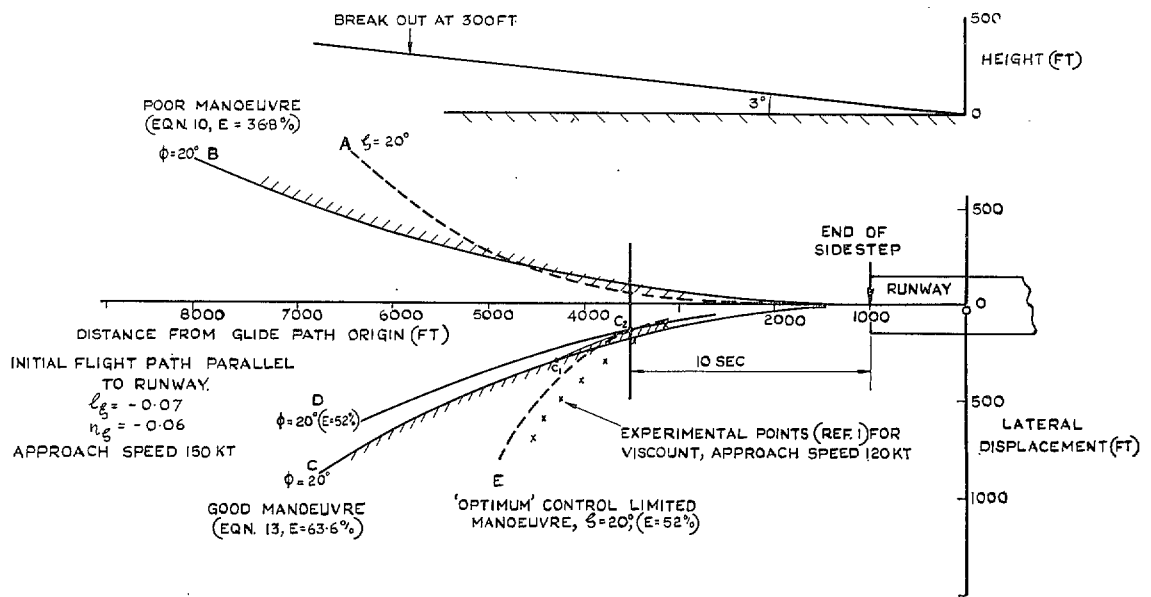FIG. 14.   Region from within which successful lateral correction manoeuvres may be achieved.

28

Publications of the
Aeronautical Research Council

ANNUAL TECHNICAL REPORTS OF THE AERONAUTICAL
RESEARCH COUNCIL (BOUND VOLUMES)

1942 Vol.   I. Aero and Hydrodynamics, Aerofoils, Airscrews, Engines.   75s. (post 2s. 9d.)
     Vol. II. Noise, Parachutes, Stability and Control, Structures, Vibration, Wind Tunnels.   47s. 6d. (post 2s. 3d.)

1943 Vol.   I. Aerodynamics, Aerofoils, Airscrews.   80s. (post 2s. 6d.)
     Vol. II. Engines, Flutter, Materials, Parachutes, Performance, Stability and Control, Structures.
                                                                              90s. (post 2s. 9d.)

1944 Vol.   I. Aero and Hydrodynamics, Aerofoils, Aircraft, Airscrews, Controls.   84s. (post 3s.)
     Vol. II. Flutter and Vibration, Materials, Miscellaneous, Navigation, Parachutes, Performance, Plates and
               Panels, Stability, Structures, Test Equipment, Wind Tunnels.   84s. (post 3s.)

1945 Vol.   I. Aero and Hydrodynamics, Aerofoils.   130s. (post 3s. 6d.)
     Vol. II. Aircraft, Airscrews, Controls.   130s. (post 3s. 6d.)
     Vol. III. Flutter and Vibration, Instruments, Miscellaneous, Parachutes, Plates and Panels, Propulsion.
                                                                              130s. (post 3s. 3d.)
     Vol. IV. Stability, Structures, Wind Tunnels, Wind Tunnel Technique.   130s. (post 3s. 3d.)

1946 Vol.   I. Accidents, Aerodynamics, Aerofoils and Hydrofoils.   168s. (post 3s. 9d.)
     Vol. II. Airscrews, Cabin Cooling, Chemical Hazards, Controls, Flames, Flutter, Helicopters, Instruments and
               Instrumentation, Interference, Jets, Miscellaneous, Parachutes.   168s. (post 3s. 3d.)
     Vol. III. Performance, Propulsion, Seaplanes, Stability, Structures, Wind Tunnels.   168s. (post 3s. 6d.)

1947 Vol.   I. Aerodynamics, Aerofoils, Aircraft.   168s. (post 3s. 9d.)
     Vol. II. Airscrews and Rotors, Controls, Flutter, Materials, Miscellaneous, Parachutes, Propulsion, Seaplanes,
               Stability, Structures, Take-off and Landing.   168s. (post 3s. 9d.)

1948 Vol.   I. Aerodynamics, Aerofoils, Aircraft, Airscrews, Controls, Flutter and Vibration, Helicopters, Instruments,
               Propulsion, Seaplane, Stability, Structures, Wind Tunnels.   130s. (post 3s. 3d.)
     Vol. II. Aerodynamics, Aerofoils, Aircraft, Airscrews, Controls, Flutter and Vibration, Helicopters, Instruments,
               Propulsion, Seaplane, Stability, Structures, Wind Tunnels.   110s. (post 3s. 3d.)

Special Volumes

     Vol.   I. Aero and Hydrodynamics, Aerofoils, Controls, Flutter, Kites, Parachutes, Performance, Propulsion,
               Stability.   126s. (post 3s.)
     Vol. II. Aero and Hydrodynamics, Aerofoils, Airscrews, Controls, Flutter, Materials, Miscellaneous, Parachutes,
               Propulsion, Stability, Structures.   147s. (post 3s.)
     Vol. III. Aero and Hydrodynamics, Aerofoils, Airscrews, Controls, Flutter, Kites, Miscellaneous, Parachutes,
               Propulsion, Seaplanes, Stability, Structures, Test Equipment.   189s. (post 3s. 9d.)

Reviews of the Aeronautical Research Council

       1939-48   3s. (post 6d.)   1949-54   5s. (post 5d.)

Index to all Reports and Memoranda published in the Annual Technical Reports

       1909-1947   R. & M. 2600 (out of print)

Indexes to the Reports and Memoranda of the Aeronautical Research Council

       Between Nos. 2351-2449   R. & M. No. 2450   2s. (post 3d.)
       Between Nos. 2451-2549   R. & M. No. 2550   2s. 6d. (post 3d.)
       Between Nos. 2551-2649   R. & M. No. 2650   2s. 6d. (post 3d.)
       Between Nos. 2651-2749   R. & M. No. 2750   2s. 6d. (post 3d.)
       Between Nos. 2751-2849   R. & M. No. 2850   2s. 6d. (post 3d.)
       Between Nos. 2851-2949   R. & M. No. 2950   3s. (post 3d.)
       Between Nos. 2951-3049   R. & M. No. 3050   3s. 6d. (post 3d.)
       Between Nos. 3051-3149   R. & M. No. 3150   3s. 6d. (post 3d.)

HER MAJESTY'S STATIONERY OFFICE

from the addresses overleaf